

## Maximal Lyapunov exponent at crises

Vishal Mehra and Ramakrishna Ramaswamy

*School of Physical Sciences, Jawaharlal Nehru University, New Delhi 110 067, India*

(Received 13 October 1995)

We study the variation of Lyapunov exponents of simple dynamical systems near attractor-widening and attractor-merging crises. The largest Lyapunov exponent has universal behavior, showing abrupt variation as a function of the control parameter as the system passes through the crisis point, either in the value itself, in the case of an attractor-widening crisis, or in the slope, for an attractor-merging crisis. The distribution of local Lyapunov exponents is very different for the two cases: the fluctuations remain constant through a merging crisis, but there is a dramatic increase in the fluctuations at a widening crisis.

PACS number(s): 05.45.+b, 05.70.Fh

### I. INTRODUCTION

In this paper, we study the behavior of the Lyapunov exponent in systems where there are abrupt changes in the dynamics as a parameter is varied. Our interest is in exploring the typical dependence of the maximal Lyapunov exponent (MLE) on the control parameter so as to elucidate the signature of a transition in the nature of the dynamics.

In the context of dynamical systems, abrupt changes in the phase space most commonly occur at the so-called *crises* [1], which are caused by the collision of a chaotic attractor with the stable manifold of an unstable periodic orbit. The three major types of crises are distinguished by the nature of discontinuous change they induce in the chaotic attractor. At a *boundary crisis*, the chaotic attractor is suddenly destroyed and replaced by a chaotic transient as the parameter passes through its critical value. This occurs when the attractor collides with the stable manifold of an unstable periodic orbit that lies on its basin boundary. At an *interior crisis*, a sudden increase or decrease in the size of the attractor occurs when the stable manifold of an unstable periodic orbit lying within the basin of attraction of the chaotic attractor collides with it. At an *attractor-merging crisis* two or more chaotic attractors simultaneously collide with the stable manifold of an unstable periodic orbit lying on their common basin boundary, which results in the merging of the attractors.

The qualitative change in the dynamics at a crisis is reflected in the Lyapunov exponents. The case of a boundary crisis is not very interesting since the Lyapunov exponent is either zero (if the transient leads to a periodic attractor) or takes a value characteristic of the chaotic attractor onto which the trajectory ultimately lands. The variation of the MLE at typical interior and merging crises is more dramatic, and in this paper we study these phenomena in a variety of simple model systems [2–5]. In all the crises, there is a similarity in the dependence of the Lyapunov exponent on the control parameter. Our major observation is that MLE has a characteristic behavior, which is, however, distinct for the attractor-widening

and attractor-merging cases. For interior crises that terminate a periodic window the dependence of MLE on the control parameter is sigmoidal, with a *large* increase in fluctuations subsequent to the crisis. This abrupt increase in the MLE at interior crises has been observed before [6–10] in some studies of one-dimensional (1D) and 2D maps and flows. In contradistinction the MLE only has a “knee” at attractor-merging crises: after the crisis, the rate of change of the Lyapunov exponent decreases significantly. Again, in contrast to the attractor-widening case, there is no attendant increase in the fluctuations of the local Lyapunov exponents subsequent to the crisis.

In the next section we describe the phenomenology of the behavior of the MLE at crises in simple maps and other low-dimensional dynamical systems. Our results have relevance to studies of systems at phase transitions, especially as a number of recent simulations of realistic systems have looked at the Lyapunov exponent,  $K$  entropy, and related quantities as a function of temperature or other control parameters [11–13]. These considerations are discussed in relation to the present work in the concluding Sec. III.

### II. THE LYAPUNOV EXPONENT AT CRISIS

The Lyapunov exponent, which is used to characterize the degree of chaoticity of a dynamical system gives the average rate of exponential divergence of two nearby trajectories [14]. In an  $n$ -dimensional dynamical system there are  $n$  Lyapunov exponents and the system is chaotic if at least one of them is positive while for regular dynamics all Lyapunov exponents are zero or negative. We focus on the largest of these, which is most simply defined as

$$\lambda_m = \lim_{t \rightarrow \infty} \lambda_m(t) = \lim_{t \rightarrow \infty} \frac{1}{t} \lim_{d(0) \rightarrow 0} \ln \frac{d(t)}{d(0)}, \quad (1)$$

where  $d(0)$  is the initial separation between two trajectories, and  $d(t)$  is their separation after time  $t$ . A number of methods have been proposed in the literature to compute one or more of the Lyapunov exponents [11,15,16]. Here

we use the tangent space method [15], which is sufficient since we are interested primarily in the largest Lyapunov exponent.

To study transient objects like repellers or semi-attractors one can also analyze the finite-time exponents  $\lambda_m(t)$ , which are also defined in Eq. (1). The instability fluctuations on an attractor can also be studied by dividing a long ergodic trajectory in segments of size  $t$  and calculating the Lyapunov exponent  $\lambda_m(t)$  for each of these. The probability density  $P(\lambda_m(t))$  of the distribution of local Lyapunov exponents has the scaling form, for  $t \rightarrow \infty$ ,

$$P(\lambda_m(t)) \sim \exp[-t\psi(\lambda_m(t))], \quad (2)$$

where  $\psi(\lambda_m(t))$  is a concave function with its minimum equal to zero at  $\lambda_m = \lambda_m(\infty)$  [17,18]. In a highly mixing system, the time correlations of  $\lambda_m(t)$  can be ignored and then by the central limit theorem  $P(\lambda_m(t))$  is a Gaussian and  $\psi(\lambda_m)$  is parabolic. However, at crisis points the Gaussian distribution breaks down and  $\psi(\lambda_m(t))$  develops a cusp at its minimum [17,19].

### A. Interior or widening crises

We first consider the logistic map

$$x_{n+1} = rx_n(1 - x_n). \quad (3)$$

It is well known [2] that as the parameter  $r$  is increased the logistic map undergoes a period-doubling cascade terminating at the accumulation point  $r_\infty \simeq 3.5699, \dots$ . Beyond that the dynamics is mainly chaotic, punctuated at various intervals by periodic windows of arbitrarily high period. A period- $n$  window is created at a saddle-node bifurcation together with an unstable period- $n$  orbit. As  $r$  is increased there is a sequence of period-doubling bifurcations creating periodic attractors of period  $2n, 2^2n, 2^3n, \dots$ . Beyond the accumulation point of the period-doubling bifurcations the attractor is made up of  $n$  distinct pieces. The trajectory hops among these

pieces in a regular manner but the distribution of points within each piece is random on the so-called semiperiodic attractor [20]. At the right end of the window there is an interior crisis when each piece of the semi-periodic attractor meets a point of the unstable period- $n$  orbit that was created in the saddle-node bifurcation, leading to an abrupt increase in the accessible phase space volume [1].

Shown in Fig. 1 is the variation of  $\lambda_m$  with  $r - r_c^n$  near the  $n = 3, 5$ , and 7-band crises, which occur at parameter  $r = r_c^n$ , respectively. We observe that for all interior crises the MLE vs  $r - r_c^n$  curve is sigmoidal. The standard deviation in the local Lyapunov exponent (calculated from  $N = 10^4$  with 50 different initial conditions) increases dramatically at the crisis. It is easy to see why the fluctuation in the local exponents should increase abruptly at the interior crises: the attractor gains large volume, which may have entirely different stability properties [10,20]. The MLE increases at the crisis because the attractor engulfs the coexisting repeller. This repeller is the remnant of the chaotic attractor, which had ceased to exist at the saddle-node bifurcation. Computation of a finite-time Lyapunov exponent near crisis shows that the repeller has larger finite-time Lyapunov exponent than the semiperiodic attractor [9]. The spectrum of local Lyapunov exponents of the postcritical attractor just before and after the three-band crisis is shown in Fig. 2(a). The linear segments indicating nonhyperbolicity at the crisis are present on both sides of  $r_c$ . After the crisis a kink at large  $\lambda$  is visible which corresponds to the distribution on the repeller [17].

Pompe and Leven [9] argued that the increase in MLE is proportional to the probability density on the repeller, and model it by the power law

$$P_R \sim (r - r_c)^\mu. \quad (4)$$

We confirm that the increase in MLE is proportional to the probability density on the repeller. A power-law fit to MLE data gives the exponent  $\mu = 0.51 \pm 0.04$  for three-band crisis and  $\mu = 0.52 \pm 0.04$  for 5 and 7 band

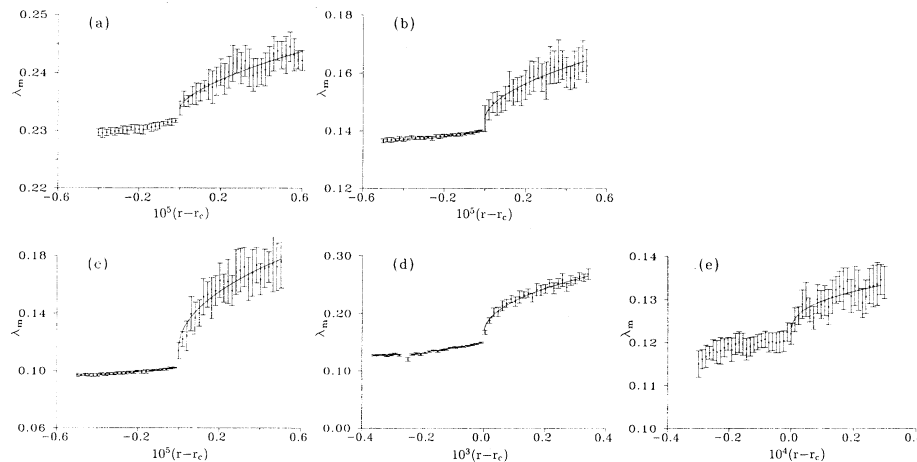


FIG. 1. Variation of the maximal Lyapunov exponent,  $\lambda_m$ , vs  $r - r_c$  around interior crises. The error bars show the magnitude of the fluctuation in the local Lyapunov exponent. Beyond the crisis, the solid line through the data is the power law  $(r - r_c)^\mu$ , with  $\mu = 0.5$  for (a), (b), and (c), and  $\mu = 0.44$  for (d) and 0.37 for (e). (a) 3-band crisis in logistic map at  $r_c^3 = 3.8568007$ . (b) 5-band crisis in the logistic map at  $r_c^5 = 3.7447104$ . (c) 7-band crisis in the logistic map at  $r_c^7 = 3.70279404$ . (d) 5-band crisis in the Kariotis-Suhl-Eckmann map at  $r_c^5 = 5.2505109$ . (e) 7-band crisis in the Hénon map at  $r_c^7 = 1.2716856$ ,  $b$  is fixed at 0.3.

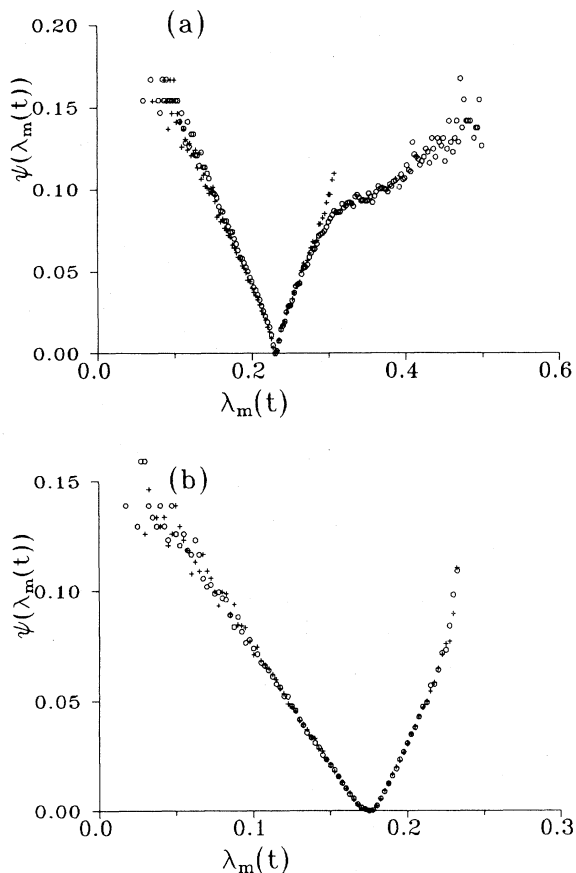


FIG. 2. Spectrum of local Lyapunov exponents,  $\psi(\lambda(n))$ , just before and after a crisis, for logistic map (a) the 3-band crisis  $r = r_c^3 \pm \delta r$ . (b) The  $m = 2$  band merging  $r = r_m \pm \delta r$ . Here  $n = 60$  and the number of iterations of the map is  $3 \times 10^6$ .  $\delta r = 1 \times 10^{-6}$ . Crosses refer to data before crisis and circles to data after crisis.

crises. Indeed, Grebogi, Ott, and Yorke [21] obtained an approximate scaling near  $r_c^3$ ,

$$P_R \sim (r - r_c^3)^{1/2} g(\ln(r - r_c^3)), \quad (5)$$

where  $g$  is a periodic function. It therefore appears that this scaling relation is valid at all other band crises as well.

Other 1D maps also show the same phenomenology. We have studied a map originally introduced by Kariotis, Suhl, and Eckmann [3] in order to mimic the dynamical behavior of intramolecular processes and isomerization. This map is given as

$$x_{n+1} = rx_n(\omega^3 - 2\omega x_n^2 + x_n^4). \quad (6)$$

We fix  $\omega = 0.8$  and consider  $r$  as the control parameter. The above map shows both attractor-merging (discussed below) and attractor-widening crises. At the 5-band crisis at  $r_c^5 = 5.2505109\dots$ , as shown in Fig. 1, it is clearly shown that the behavior of the Lyapunov exponent is essentially identical to that observed for the logistic map.

Higher-dimensional systems also show the same behavior: for example, the well-known Hénon map,

$$\begin{aligned} x_{n+1} &= y_n + 1 - rx_n^2, \\ y_{n+1} &= bx_n, \end{aligned} \quad (7)$$

which has a well-characterized, complex structure of bifurcations and crises [14]. Fixing  $b=0.3$  and varying  $r$ , the 7-band crisis occurs at  $r_c^7 = 1.2716856$ . Again (cf. Fig. 1) it is seen that the maximal Lyapunov exponent shows the by now familiar characteristic sigmoidal behavior as the function of  $r - r_c^7$ .

### B. Attractor-merging crises

Attractor-merging crises typically occur because of some symmetry in the underlying dynamics, for example, in the logistic map, beyond the accumulation point of the period-doubling cascade  $r_\infty$  there is a successive

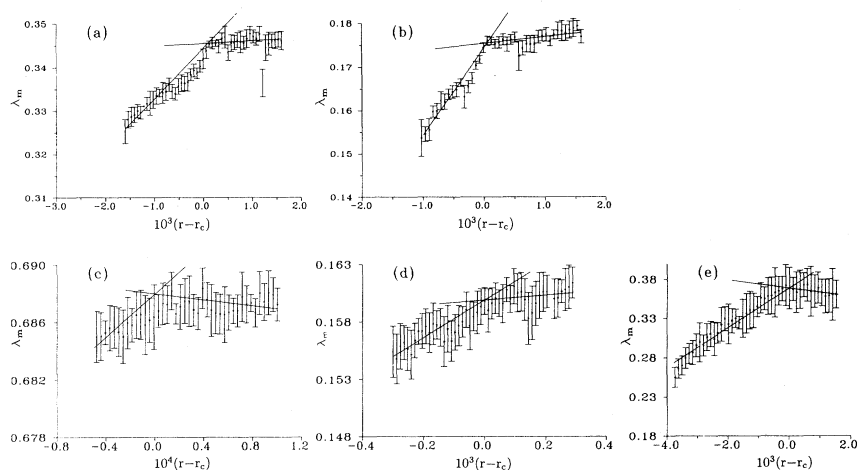


FIG. 3. Variation of the maximal Lyapunov exponent,  $\lambda_m$ , vs  $r - r_c$  around attractor-merging crises. As in Fig. 1 the error bars show the magnitude of the fluctuation in the local Lyapunov exponent. The straight lines through the data are a least-square fit constrained to pass through the critical point. (a)  $m = 2$  band merging in the logistic map at  $r = 3.678486$ . (b)  $m = 1$  band merging in the logistic map at  $r = 3.59256296$ . (c) Attractor merging in Kariotis-Suhl-Eckmann map at  $r = 5.7409035$ . (d) Hénon map merging crisis at  $r = 1.084404$ ,  $b$  is again fixed at 0.3. (e) Well merging in the forced Duffing equation at  $r \approx 0.853$ .

merging of chaotic bands. Thus, for  $r < r_m$  the chaotic attractor consists of  $2^m$  chaotic bands. If we take a point in any one of these  $2^m$  bands the trajectory will come to that band after  $2^m$  iterations, so that the band can be considered as an attractor for the  $2^m$ -times iterated map and the band-merging phenomenon can be regarded as an attractor-merging crisis [1] for the  $2^m$ -times iterated map.

We show results for the  $m = 1$  merging at  $r_m = 3.678486\dots$  and the  $m = 2$  merging at  $r_m = 3.5925663\dots$  in Fig. 3. For band-merging crises the MLE vs  $r - r_m$  curve has a sharp *knee* precisely at  $r = r_m$ , i.e., the derivative of MLE is discontinuous at  $r_c$ . However, the knee angle is not the same for all band mergings. The local Lyapunov exponents are more uniform here, and we do not see any significant change in the fluctuation properties after the crisis. This is not difficult to understand as the co-merging attractors are symmetry related. Similar behavior was observed for attractor mergings in the other maps studied [3,4] [Fig. 3]. The spectrum of local Lyapunov exponents near the attractor-merging crisis [Fig. 2(b)] shows the linear segments indicative of the nonhyperbolicity at the crisis [19].

We also consider a merging crisis in the forced Duffing equation [1]:

$$d^2x/dt^2 + \nu dx/dt + \alpha x^3 - \beta x = r \sin \omega t. \quad (8)$$

We take  $\nu = 1, \alpha = 100, \beta = 10, \omega = 3.5$ , and study Eq. (8) near its crisis value  $r_m = 0.853$ . Below  $r_m$  there are two chaotic attractors, one confined to the well in  $x > 0$  and another confined to the well in  $x < 0$ . These attractors merge at  $r = r_m$ , where the MLE near  $r = r_m$  again shows a knee (Fig. 3).

### III. CONCLUSIONS

In this work we have studied the variation of the largest Lyapunov exponent MLE near interior and attractor-merging crisis for some simple and well-known systems.

We observe that around an interior crisis, the MLE vs the control parameter curve has a sigmoidal dependence, with the fluctuations increasing dramatically at the crisis. For the 3-band crisis in the logistic map (Fig. 1), for example, the average fluctuation just before the crisis is  $4.2 \times 10^{-4}$ , while after the crisis it is  $1.2 \times 10^{-3}$ . On the other hand, a knee-shaped curve is observed for the attractor-merging crises with no increase in fluctuations beyond crisis.

In recent work Fan and Chay [22] have studied the Lyapunov exponents of Rose-Hindmarsh system (consisting of three coupled differential equations), and report that Lyapunov exponents are not good indicators of an interior crisis. They prefer the use of topological entropy,

which showed an abrupt increase at the crisis. However, in contrast to the present systems where the interior crises terminate a periodic window the interior crisis they studied was caused by collision of two period-adding bifurcation processes traveling in opposite directions in the parameter space. This may be one reason why they did not observe an increase in the MLE at the crisis.

The observations made above are of relevance to recent simulation studies of systems undergoing a change in bulk phase. In recent years it has become possible to study the detailed dynamics of mesoscopic systems undergoing phase change, and a number of studies [11–13] have therefore focused on the relation between phase transitions and the Lyapunov exponents that characterize the dynamics. For example, in a study of a large number of coupled planar rotors, Butera and Caravati [12] found a discontinuity in the slope of the maximal Lyapunov exponent (MLE) at the precise temperature of the Kosterlitz-Thouless transition. More recently, it has been seen in molecular-dynamics simulations of small Lennard-Jones clusters [13] that the largest Lyapunov exponent also increases dramatically as the system makes a transition from a solidlike to a liquidlike phase. This abrupt change characterizes the phase transition in a manner exactly analogous to the Lindemann criterion, and indeed offers an alternative connection between the phase space dynamics and the phase change.

This abrupt increase in the MLE corresponds to an increase in the available phase space volume and consequently in the local rate of divergence of trajectories [15]. Berry and co-workers [11] have looked at a variety of dynamical indicators, including the Kolmogorov-Sinai entropy, i.e., the sum of all positive Lyapunov exponents. This quantity increases smoothly with temperature or energy as the phase changes although information can be obtained regarding underlying potential-energy surfaces [11].

The present study further underscores the utility of the MLE as an indicator of phase transformation since the band crises between different chaotic phases are, in a sense, dynamical system analogues of phase transitions. Prior to the crisis there is long-time correlated noisy periodicity while after the crisis, dynamics lacks long-time correlation since motion is chaotic within a single-band attractor.

### ACKNOWLEDGMENTS

This work was supported by Grant No. SPS/MO-5/92 from the Department of Science and Technology, and the CSIR, India. We also thank C. Chakravarty for comments on the manuscript.

- 
- [1] C. Grebogi, E. Ott, Romeiras, and J. A. Yorke, Phys. Rev. A **36**, 5365 (1987).  
 [2] R. M. May, Nature **261**, 459 (1976).  
 [3] R. Kariotis, H. Suhl, and J. P. Eckmann, Phys. Rev. Lett.

- 54**, 1106 (1985).  
 [4] M. Hénon, Commun. Math. Phys. **50**, 69 (1976).  
 [5] J. Gukenheimer and P. Holmes, *Nonlinear Oscillations, Dynamical Systems and Bifurcations of Vector Fields*,

- (Springer, New York, 1983).
- [6] R. W. Leven and B. P. Koch, *Phys. Lett. A* **86**, 71 (1981).
  - [7] R. W. Rollins and E. R. Hunt, *Phys. Rev. A* **29**, 3327 (1984).
  - [8] E. G. Guinn and R. M. Westervelt, *Phys. Rev. A* **33**, 4143 (1986).
  - [9] R. Pompe and R. W. Leven, *Phys. Scr.* **38**, 651 (1988).
  - [10] K. G. Szabo and T. Tél, *Phys. Lett. A* **196**, 173 (1994).
  - [11] T. L. Beck, D. M. Leitner, and R. S. Berry, *J. Chem. Phys.* **89**, 1681 (1988); R. J. Hinde, R. S. Berry, and D. J. Wales, *J. Chem. Phys.* **96**, 1376 (1992).
  - [12] P. Butera and G. Caravati, *Phys. Rev. A* **36**, 962 (1987).
  - [13] S. Nayak, R. Ramaswamy, and C. Chakravarty, *Phys. Rev. E* **51**, 3376 (1995).
  - [14] A. J. Lichtenberg and M. A. Lieberman, *Regular and Chaotic Dynamics* (Springer-Verlag, Berlin, 1992).
  - [15] G. Benettin, L. Galgani, and J. M. Strelcyn, *Phys. Rev. A* **14**, 2338 (1976).
  - [16] I. Shimada and T. Nagashima, *Prog. Theor. Phys.* **61**, 1605 (1979).
  - [17] S. Miyazaki, N. Mori, T. Yoshida, H. Mori, H. Hata, and T. Horita, *Prog. Theor. Phys.* **82**, 863 (1989).
  - [18] P. Grassberger, R. Badii, and A. Politi, *J. Stat. Phys.* **51**, 135 (1988).
  - [19] K. Tomita, H. Hata, T. Horita, H. Mori, and T. Morita, *Prog. Theor. Phys.* **80**, 953 (1988).
  - [20] B. E. Kendall, W. M. Schaffer, and C. W. Tidd, *Phys. Lett. A* **177**, 13 (1993).
  - [21] C. Grebogi, E. Ott, and J. A. Yorke, *Physica* **7D**, 181 (1983).
  - [22] Y. S. Fan and T. R. Chay, *Phys. Rev. E* **51**, 1012 (1995).